Available online at www.sciencedirect.com
ScienceDirect
Journal of Photochemistry and Photobiology A: Chemistry 184 (2006) 273–281
Journal of Photochemistry and Photobiology A:Chemistry
www.elsevier.com/locate/jphotochem

Adsorbed species on TiO_2 associated with the photocatalytic oxidation of trichloroethylene under UV

Soon-Kil Joung *, Takashi Amemiya, Masayuki Murabayashi, Kiminori Itoh

Graduate School of Environment and Information Sciences, Yokohama National University, 79-7 Tokiwadai, Hodogaya-ku, Yokohama 240-8501, Japan

Received 3 September 2005; received in revised form 6 February 2006; accepted 29 April 2006
Available online 7 May 2006

Abstract

Fourier Transform Infrared (FT-IR) spectroscopy and X-ray photoelectron spectroscopy (XPS) were used to investigate the species adsorbed on TiO_2 related to photocatalytic activity. Dichloroacetyl chloride (DCAC), which is generated during the photocatalytic oxidation of trichloroethylene (TCE), was the only species adsorbed on TiO_2. Two types of DCAC were adsorbed – one at low concentration and another at high concentration. While adsorbed phosgene produced from DCAC was adsorbed strongly to TiO_2, the adsorption of DCAC was relatively weak. The surface structures of the adsorbed DCAC at low and high concentrations on TiO_2 were carboxylate compounds on single Ti–O bonds. The surface structures of carboxylate compounds were resolved to those of adsorbed phosgene, bidentate carbonate compounds, on the two Ti–O bonds during photocatalytic oxidation under UV irradiation. The adsorbed DCAC on TiO_2 reduces the photooxidation rate of TCE, and the $CHCl_2$ stretching vibration of adsorbed DCAC was considered to be the inactive species. The adsorbed DCAC and dichloroacetic acid (DCAA) were converted to adsorbed phosgene by photocatalytic oxidation on TiO_2.

Keywords: Adsorbed species; DCAC; Phosgene; TCE; TiO_2; Photocatalyst; Surface

1. Introduction

TiO_2 photocatalysts have been used extensively for both interior and environmental cleaning, and for solar energy conversion [1,2]. TiO_2, which is used as a photocatalyst, has attracted a great deal of attention since the early 1990s because of the effect of photocatalytic oxidation of gaseous TCE [3], and because of its lack of toxicity, relative inexpensiveness, high level of activity, and chemical stability [2]. Thus, large numbers of commercial goods associated with these photocatalysts have been developed and are used in both daily life and in industry. There have been a number previous studies of photocatalysts, such as investigations of their preparation methods [4] and their reaction mechanisms [5]. However, such basic studies of photocatalysts are still insufficient to compare to applied studies. In particular, although the photocatalytic reaction occurs on the surface of TiO_2, there is still controversy regarding the adsorbed species and the active species on TiO_2 [6–8].

For example, TCE, a well-known volatile chlorinated organic compound (VCOC), has been used as an industrial solvent for degreasing and dry cleaning and has become one of the most common environmental contaminants [9]. Hence, while TCE cleaning technology has been developed [10], the TCE photocatalytic degradation reactions on adsorbed species and active species have not yet been clarified. In the photocatalytic oxidation of TCE, the active species on its surface are known to include OH radicals, chlorine radicals, and active oxygen species. The OH radical and oxygen radical ($^{\bullet}O$) are known to be initiators of the oxidation reaction [5,6,11–13]. These radicals are produced through the following pathways (reactions (1)–(4)) [7,14,15]:

$$TiO_2 \overset{h\nu}{\rightleftarrows} h^+ \ (VB) + e^- \ (CB) \quad (1)$$

$$h^+ \ (VB) + OH^- \rightarrow {}^{\bullet}OH \ (oxidationreaction) \quad (2)$$

$$e^- \ (CB) + O_2 \rightarrow O_2{}^- \ (reductionreaction) \quad (3)$$

$$O_2{}^- + h^+ \ (VB) \rightarrow 2{}^{\bullet}O \ (oxidationreaction) \quad (4)$$

*VB, valence band; CB, conduction band.

The Cl radical produced through several pathways has been shown to be the species involved in the TCE chain reaction

* Corresponding author. Tel.: +81 45 339 4354; fax: +81 45 339 4354.
E-mail address: joungskynu@yahoo.co.jp (S.-K. Joung).

1010-6030/$ – see front matter © 2006 Elsevier B.V. All rights reserved.
doi:10.1016/j.jphotochem.2006.04.040

[16,17], and it has been shown to play a key role in the photocatalytic oxidation of TCE along with both adsorbed and gas-phase oxygen [18,19]. However, as the chlorine ion on the TiO_2 surface is also known to poison the catalyst, further detailed studies of the adsorption state of chlorine on TiO_2 are necessary. Thus, the reaction mechanism of TCE on the active species is still under investigation, and no complete interpretation has yet been formulated [8].

DCAC and phosgene are the main gas-phase intermediates formed during the photocatalytic oxidation of gas-phase TCE on TiO_2 [5,20–22]. The adsorbed species on TiO_2 were also shown to be DCAC and phosgene [6]. The infrared bands of the adsorbed DCAC and the adsorbed phosgene showed peaks at 1581, 1418, 1228, and 1650 cm^{-1} (shoulder), and showed a peak at 1740 cm^{-1}, respectively [6]. However, in our previous study, no infrared band of phosgene chemically adsorbed on TiO_2 was observed near 1740 cm^{-1} using Fourier Transform Infrared (FT-IR) [23]. Hence, further investigations are required to identify the adsorbed species on TiO_2 during TCE photooxidation.

In the present study, we investigated the species adsorbed on TiO_2 during TCE photooxidation using FT-IR.

Commercial DCAC, commercial DCAA, and prepared phosgene [23], considered as standard compounds, were used for comparison with the species adsorbed on TiO_2 during TCE photooxidation. We also performed quantitative and qualitative analysis of the species adsorbed on TiO_2 by X-ray photoelectron spectroscopy (XPS). Based on the results of the present study, we propose the surface structure for adsorbed species on TiO_2.

2. Experimental

2.1. Silicon wafers coated with titanium dioxide and general procedure

Silicon wafers were first cut to a size of approximately 18 mm × 18 mm, and then cleaned with hydrofluoric acid (46%) and acetone (99.5%) for 20 min each in an ultrasonic cleaning machine, followed by drying for 10 min at 373 K. This procedure was carried out to remove the impurities adsorbed on the surface of the silicon wafers. Silicon wafers coated with TiO_2 (Si–TiO_2) were prepared by dipping them into TiO_2 sol (STS-01; Ishihara Sangyo Kaisha Ltd., Tokyo, Japan). To remove physisorbed water on the surface TiO_2, samples were heated at 723 K for 3.5 h under a stream of N_2 gas (ultra-high purity, 99.9995%). The TiO_2 was still in the anatase crystalline form. After heating, the samples were cooled to room temperature under a stream of N_2 gas. The Si–TiO_2 wafer samples were placed on the sample holder, which was then set in the center of the two injection ports on the reactor under an atmosphere of N_2 gas. In addition, UV pre-illumination was performed for 30 min on the Si–TiO_2 wafer set inside the reactor, and photoproducts (such as water) generated were subsequently removed by replacing with dry air. UV pre-illumination was repeated until no more water was removed. Measurements using FT-IR were performed under an atmosphere of N_2 gas.

A Pyrex glass cylinder (internal volume, 60.5 mL) was used as the reactor for IR measurements, and was equipped with barium fluoride (BaF_2) windows that transmit infrared signals at both ends. Two injection ports on the cell allowed the introduction of replacement gas (dry air or N_2 gas) and the reactants, such as TCE, DCAC, DCAA, and phosgene. This infrared cell reactor can be employed for measurement of the infrared spectra of the adsorbed species on the TiO_2 surface and/or of the gas-phase species inside the cell. Dry air or N_2 gas was used to pretreat impurities on the catalytic surface and to remove gas-phase species inside the reactor.

2.2. The adsorbed species on TiO_2 and the photocatalytic oxidation of TCE

The photocatalytic oxidation of TCE was carried out at low (7.2×10^{-5} mol/L) and high (3.6×10^{-4} mol/L) concentrations under UV irradiation. Prior to removal of the gas-phase species, the byproducts inside the cell were considered to coexist with the gas-phase and adsorbed species (gas-phase/adsorbed species) on TiO_2. After removal of the gas-phase species by replacement with dry air or N_2 gas, only surface species on TiO_2 will be detected by FT-IR spectroscopy (Nicolet 800 FT-IR Spectrometer; Thermo Electron K.K., Yokohama, Japan). XPS was used to analyze the adsorbed species on TiO_2 by XSAM-800 (Kratos Analytical Ltd., Hadano, Japan) after analysis by FT-IR. Gas chromatography–mass spectrometry (GC/MS; Hewlett-Packard 6890/5973, Hewlett-Packard, Palo Alto, CA) was used to observe the product generated from photocatalytic oxidation of TCE with different concentration. Eight fluorescent black light blue lamps (UV-BLB, Toshiba FL20S.BLB, total intensity = 3.8 mW cm^{-2}) with a peak wavelength of 352 nm (300–425 nm) were employed as UV sources. The fluorescent lamps were arranged symmetrically in a cylindrical metallic container (60 cm in length and 35 cm in diameter) equipped with a fan to minimize the effect of heating caused by UV irradiation.

Standard DCAC (97%) and standard DCAA (99%) purchased from Junsei Chemical Co., Ltd. (Tokyo, Japan) and standard phosgene prepared as described previously [23] were adsorbed onto the surface of TiO_2 at different concentrations to allow comparison with the adsorbed species on TiO_2 during TCE photooxidation. These adsorbed species were photocatalytically oxidized on TiO_2 and analyzed by FT-IR and XPS under the experimental conditions described above.

3. Results

3.1. Assignment of adsorbed species on the TiO_2 surface during photocatalytic oxidation of TCE with thin TiO_2 films

The infrared spectra shown in Fig. 1 are those of the byproducts generated during photocatalytic oxidation of TCE. In general, although the infrared bands of gas-phase DCAC were observed at 1820 and 1788, 1225, 1076 and 989 cm^{-1}, and 800 and 741 cm^{-1}, corresponding to the C=O stretch, C–H stretch, C–C stretch, and C=Cl_2 stretch, respectively, and although infrared bands of gas-phase phosgene were observed at 1832 and 1820, 1682, 856 and 848, and 1008 cm^{-1}, corresponding to the C=O stretch, 2 (C–Cl_2) bend, C–Cl_2 bend, and

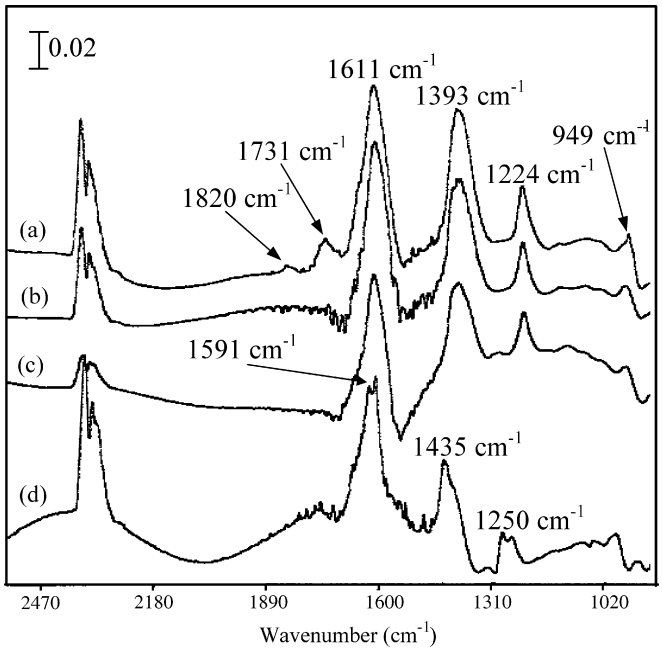

Fig. 1. Infrared spectra associated with byproducts generated during the photocatalytic oxidation of TCE: (a) gas-phase and adsorbed species produced during photocatalytic oxidation of TCE at low concentration (7.2×10^{-5} mol/L); (b) only adsorbed species formed on the TiO_2 surface; (c) species adsorbed with standard DCAC (1.67×10^{-5} mol/L); (d) species adsorbed with standard DCAA (7.93×10^{-5} mol/L). The oxidation time with UV irradiation as shown in (a) was 3 min.

unreported, respectively [11,24,25], the infrared bands of gas-phase/adsorbed species detected during photocatalytic oxidation of TCE at low concentration (7.2×10^{-5} mol/L) (Fig. 1(a)) were observed at 1820, 1731, 1611, 1393, 1224, and 949 cm^{-1} involving infrared bands of DCAC and phosgene also detected on measurement by GC/MS.

The infrared spectrum shown in Fig. 1(b) is merely that of the adsorbed species on the TiO_2 surface, and was obtained by removing the gas-phase species by replacing them inside the cell with dry air under the conditions shown in Fig. 1(a). While the infrared spectrum shown in Fig. 1(b) is very similar to that of the standard adsorbed DCAC shown in Fig. 1(c), it was very different from that of the standard adsorbed DCAA shown in Fig. 1(d). These results indicated that the species adsorbed on the TiO_2 surface during photocatalytic oxidation of TCE was DCAC and not DCAA.

At low concentration, infrared bands of species adsorbed during TCE photooxidation were observed at 1611, 1393, and 1224 cm^{-1} as the main species, corresponding to the COO asymmetric stretch, the COO symmetric stretch, the $CHCl_2$ stretching vibration, respectively, and bands of the other species were also observed near 1645 and 942 cm^{-1}. In addition, as the bands of the gas-phase species were few and of low intensity, as shown in Fig. 1(a), we performed photocatalytic oxidation of TCE at high concentration (3.6×10^{-4} mol/L).

Fig. 2 shows the infrared spectra associated with byproducts generated during photocatalytic oxidation of TCE at high concentration: (a) the gas-phase/adsorbed species; (b) only the adsorbed species; (c) standard adsorbed DCAC at high concentration. As shown in Fig. 2(a), the infrared bands observed near 1820, 856, and 848 cm^{-1} were assigned to phosgene, and those observed near 1820, 1789, 1731, 1645 (shoulder), 1611, 1393, 1224, 1075, and 989 cm^{-1} were assigned to DCAC. After removal of the gas-phase species by replacing them inside the cell with dry air, as shown in Figs. 2(b) and 2(c), the infrared

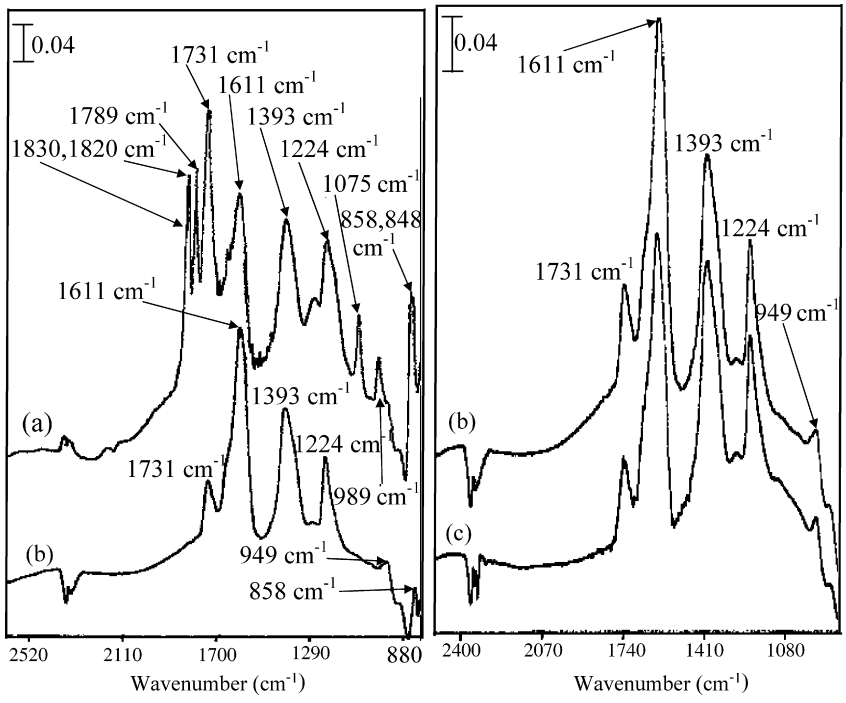

Fig. 2. Infrared spectra of byproducts generated during the photocatalytic oxidation of TCE at high concentration (3.6×10^{-4} mol/L): (a) gas-phase and adsorbed species; (b) only adsorbed species formed on the TiO_2 surface; (c) species adsorbed with standard DCAC (6.67×10^{-5} mol/L). The oxidation time with UV irradiation was 8 min.

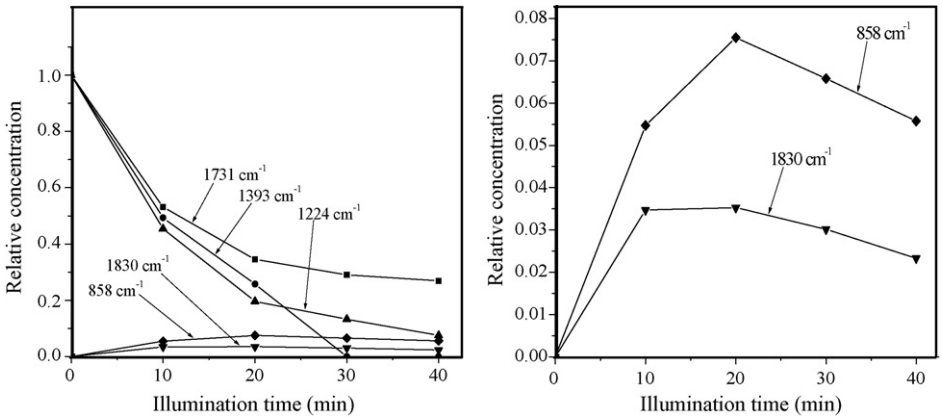

Fig. 3. (Left panel) Changes in the intensities by photocatalytic oxidation of DCAC adsorbed on TiO_2 at high concentration. (Right panel) An enlarged view of the peaks at 1830 and 858 cm^{-1} on the left panel.

bands of the adsorbed species alone were observed at 1611, 1393, 1224, and 1731 cm^{-1} as the main adsorbed species, and bands of the other species were also observed near 1645 and 942 cm^{-1} as observed at low concentration.

While the infrared band of 1731 cm^{-1} was not observed for the adsorbed species during TCE photooxidation at low concentration or DCAC adsorbed on TiO_2 at low concentration with standard compounds, this infrared band was observed for the adsorbed species during TCE photooxidation at high concentration and for DCAC adsorbed at high concentration with standard compounds. Therefore, we assigned the infrared band of 1731 cm^{-1} in the gas-phase/adsorbed species (Fig. 2(a)) and in the adsorbed species alone (Fig. 2(b)) to adsorbed DCAC, because the infrared spectrum (Fig. 2(b)) was very similar to that of standard adsorbed DCAC (Fig. 2(c)). However, Driessen et al. reported this band to be adsorbed phosgene [6].

We continued our investigation to assign the infrared band observed at 1731 cm^{-1} via photocatalytic oxidation of the species adsorbed on the surface of TiO_2. Fig. 3 shows the results of photocatalytic oxidation of the species adsorbed on TiO_2 during TCE photooxidation at high concentration, as shown in Fig. 2(b). The intensities of the peaks at 1393, 1224, and 1731 cm^{-1} decreased with progression of the photocatalytic oxidation of adsorbed DCAC. However, the intensities of the bands at 858 and 1830 cm^{-1}, well known to be phosgene, increased with the progression of photocatalytic oxidation of adsorbed

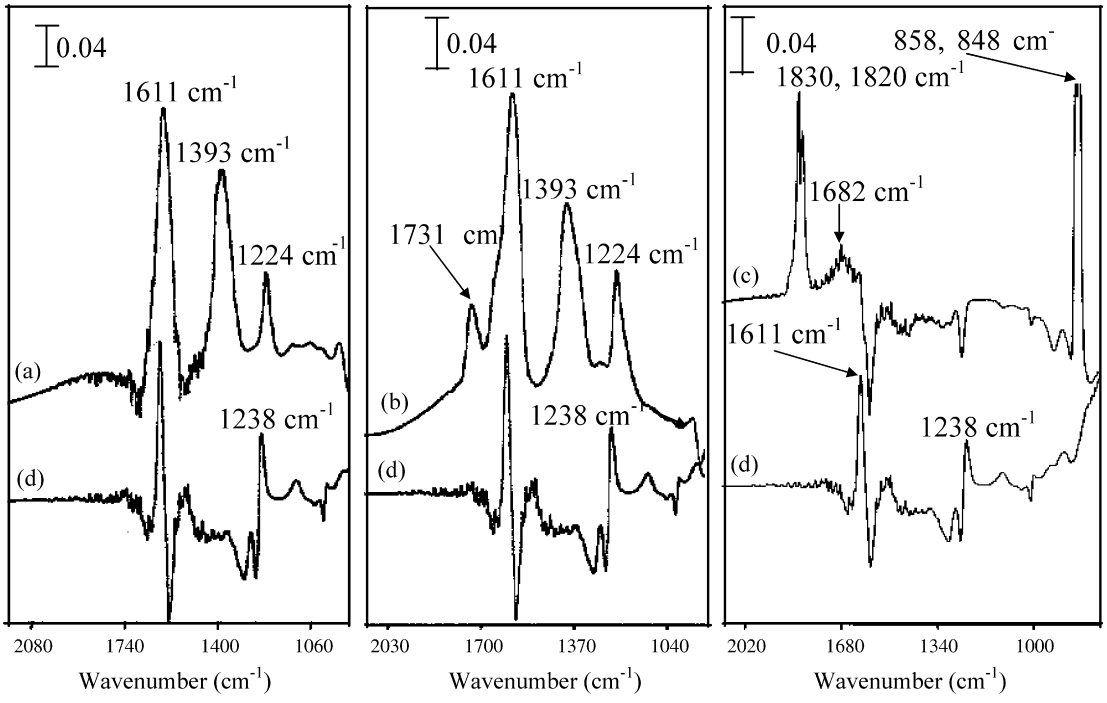

Fig. 4. Infrared spectra of (left panel) (a) the surface species adsorbed on TiO_2 during TCE photooxidation at low concentration (7.2×10^{-5} mol/L), (center panel), (b) the surface species adsorbed after TCE photooxidation at high concentration (3.6×10^{-4} mol/L), (right panel), (c) the gas-phase and adsorbed phosgene on TiO_2, and (d) only the adsorbed phosgene on TiO_2. Phosgene concentration introduced for adsorption on TiO_2 was 4.52×10^{-6} mol/L.

DCAC. If the peak at 1731 cm^{-1} could be assigned to phosgene, it should have increased. However, as the band at 1731 cm^{-1} decreased, we considered this peak to most likely be due to DCAC species adsorbed at high concentration.

Next, Fig. 4 shows a comparison of the infrared spectra of the standard adsorbed phosgene with that of the surface species adsorbed on TiO_2 during photocatalytic oxidation of TCE at low and high concentrations. While the band at 1731 cm^{-1} was not observed for the species adsorbed during TCE photooxidation at low concentration (Fig. 4(a)) or for standard adsorbed phosgene (Fig. 4(d)), it was observed for the species adsorbed during TCE photooxidation at high concentration. In particular, the panel on the right shows the infrared spectra of the gas-phase/adsorbed species (c) and the adsorbed species alone (d) of standard phosgene; no band was observed at 1731 cm^{-1} in the infrared spectra of standard adsorbed phosgene. With the exception of the infrared band at 1611 cm^{-1}, the remaining bands were also very different from those of DCAC adsorbed at low and high concentrations. Therefore, we determined that the band at 1731 cm^{-1} was also not adsorbed phosgene but was the DCAC species adsorbed at high concentration. Hence, we studied the possible existence of a different adsorbed structure at low and high concentrations.

Furthermore, we found no significant differences in adsorbed species, such as a shift or new generation, by replacing materials, such as dry air and N_2 gas. We also found no influence of BaF_2 windows on the detection of adsorbed species after removal of gas-phase species by replacement with dry air or N_2 gas. Thus, the removal of gas-phase species by replacement with dry air or N_2 gas was considered to be efficient for the observation of adsorbed species on TiO_2.

3.2. The number of adsorbate structure-types

We studied the concentration dependence for each band of DCAC adsorbed at different concentrations, as shown in Fig. 5. These plots were obtained from the integrated intensities of the infrared bands of the adsorbed species, which were based on

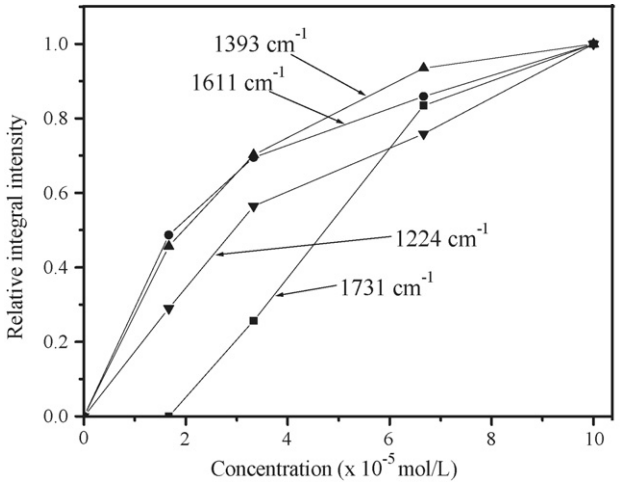

Fig. 5. Changes in integrated intensity for the infrared bands of DCAC species adsorbed at different concentrations.

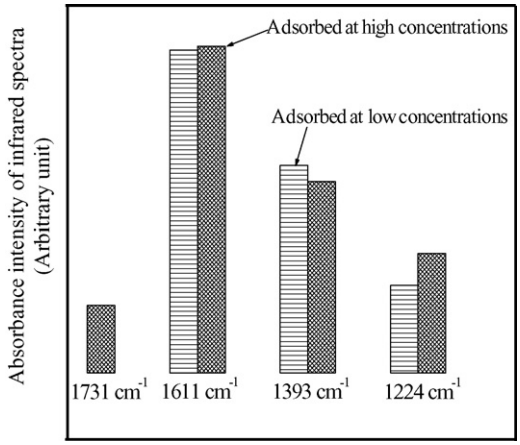

Fig. 6. Comparison of absorbance intensities for surface species adsorbed on TiO_2 during photocatalytic oxidation of TCE at low and high concentrations.

bands at 1731, 1611, 1393 and 1224 cm^{-1}. Each plot was normalized at the beginning or the end for ease of comparison. The integrated intensity of 1731 cm^{-1} was significantly different from those of the other bands. With the exception of the band at 1731 cm^{-1}, the rest of the infrared bands were observed even at low concentration (7.2×10^{-5} mol/L). These observations suggested that there are different adsorbed structures at low and high concentrations.

Next, we investigated the absorbance intensities of the infrared spectra at low and high concentrations (Fig. 4(a) and (b)). Fig. 6 shows a comparison of absorbance intensities of the species adsorbed on TiO_2 during TCE photooxidation at low and high concentrations. As shown in Fig. 6, the differences in the absorbance intensities of the bands at 1611, 1393, and 1224 cm^{-1} were very low even at low and high concentrations. However, the difference in the absorbance intensities at 1731 cm^{-1} was very high, which could not be detected at low concentration. If the absorbance intensities are dependent on concentration, the infrared band at 1731 cm^{-1} at low concentration should be proportional to that at 1731 cm^{-1} at high concentration, as observed for the other infrared bands.

In addition, we studied the adsorption isotherms of adsorbed DCAC, as shown in Fig. 6. This type usually occurs when multiple layers of gas are adsorbed onto the surface of the pores in a porous solid [26]. The gas-phase DCAC becomes so thick that it fills the pores, and eventually no more gas-phase DCAC can be adsorbed and the isotherm is saturated [26]. Although DCAC adsorbed at a low concentration may not be adsorbed in multiple layers, we considered DCAC adsorbed at a high concentration, as shown in reaction (VI) of Eq. (6), to be adsorbed in multiple layers. Furthermore, although DCAC adsorbed at a high concentration was adsorbed in multiple layers, no changes were observed in the infrared bands of DCAC adsorbed at a high concentration. Therefore, the number of adsorbed structure-types is limited only to the two types mentioned above, with and without the band at 1731 cm^{-1} at high (3.6×10^{-4} mol/L) and low concentration (7.2×10^{-5} mol/L), respectively. To investigate the existence of adsorbed structures of other types, we carried out qualitative analysis of DCAC species adsorbed on TiO_2 at low

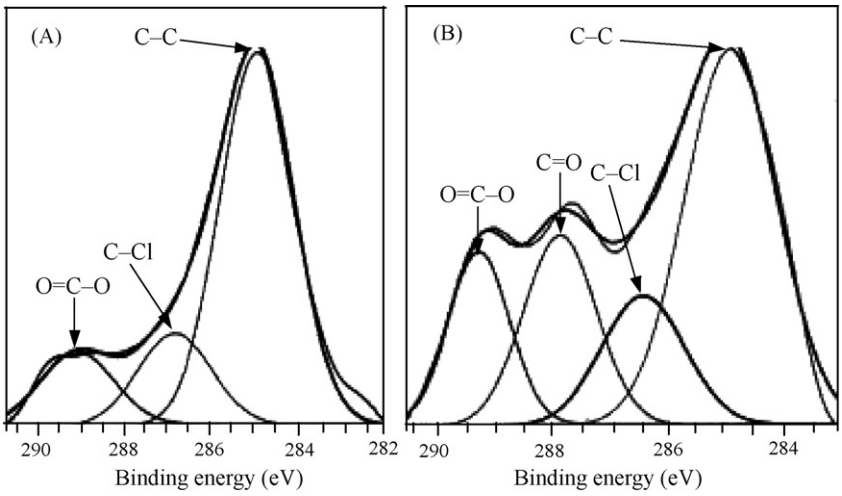

Fig. 7. The curve-resolved spectrum of the C 1s region for lens C on qualitative analysis of DCAC species adsorbed on TiO_2 by XPS. (left panel, A) Spectrum of the species adsorbed at low concentration. (right panel, B) Spectrum of the species adsorbed at high concentration.

and high concentrations by XPS (Fig. 7). Fig. 7 shows the curve-resolved spectrum of the C 1s region for lens C. The binding energies around 289.1, 284.9, 286.6, and 287.8 eV were assigned to the O=C–O, C–C, C–Cl, and C=O bonds, respectively [27,28]. As shown in Fig. 7A and B, the binding energy of the C=O bond was not observed for the DCAC species adsorbed on TiO_2 at low concentration, whereas that of the C=O bond was observed around 287.8 eV in the case of the DCAC species adsorbed on TiO_2 at high concentration. These results indicated that there are two types of adsorbed structure – one at low concentrations and another at high concentrations.

3.3. Photocatalytic oxidation of TCE in the presence of surface species adsorbed on TiO_2

We investigated the effects of the photocatalytic oxidation of TCE in the presence of DCAC adsorbed at low (1.67×10^{-5} mol/L) and high concentrations (6.67×10^{-5} mol/L). Fig. 8 shows the changes in the concentration of TCE due to photocatalytic oxidation in the presence of adsorbed DCAC at low (Line B) and at high (Line A) concentrations through the FT-IR bands. The photocatalytic oxidation of TCE was most effective when performed in the absence of adsorbed DCAC, as shown in Fig. 8C. In the adsorbed DCAC, the photocatalytic oxidation of TCE in the presence of DCAC adsorbed at low concentration was more effective than at high concentration. The photocatalytic oxidation of TCE in the presence of DCAC adsorbed at low concentration also converted that into adsorbed DCAC at high concentration involving the infrared band at 1731 cm^{-1}. Although the reaction rate of TCE was reported to be independent of the DCAC partial pressure [20], in our study and in those of other groups, the adsorbed DCAC was shown to deactivate the photocatalytic oxidation of TCE [29].

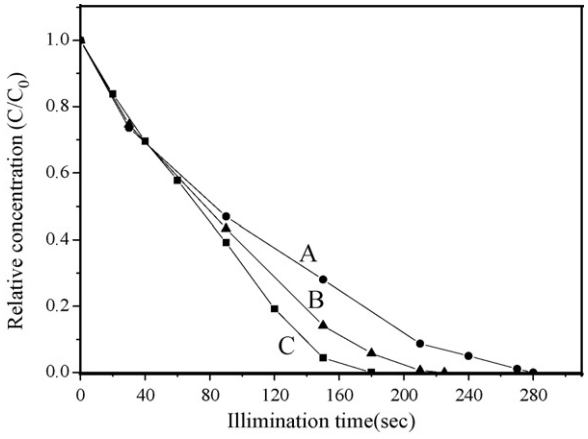

Fig. 8. Effects of photocatalytic oxidation of TCE (7.2×10^{-5} mol/L) in the presence of adsorbed DCAC: (A) in the presence of high concentration (6.67×10^{-5} mol/L); (B) in the presence of low concentration (1.67×10^{-5} mol/L); (C) in the absence of adsorbed species.

Hence, we investigated the active species of DCAC adsorbed on TiO_2, as determined by quantitative analysis using XPS and as shown in Table 1. While the adsorbed DCAC at low concentration contained little chlorine as compared with that at high concentration, the photocatalytic oxidation rate of TCE in the presence of adsorbed DCAC at low concentration was more marked than that at high concentration, and the ratio of apparent quantum yield was about 1.3-fold, as shown in Fig. 8. One reason is that the $CHCl_2$ stretching vibration of DCAC adsorbed on TiO_2 may deactivate the photocatalyst, as described in Section 4. As Cl radicals and Cl ions are known to contribute to chain reactions and act as a catalyst poison, respectively [30,31], further

Table 1
Results of quantitative analysis of surface species on TiO_2 during TCE photooxidation by XPS

Sample condition	Contents of the analyzed elements (%)			
	Ti 2p	C 1s	O 1s	Cl 2p
DCAC adsorbed at a low concentration	22.78	15.26	61.31	0.59
DCAC adsorbed at a high concentration	22.11	12.57	62.44	2.9

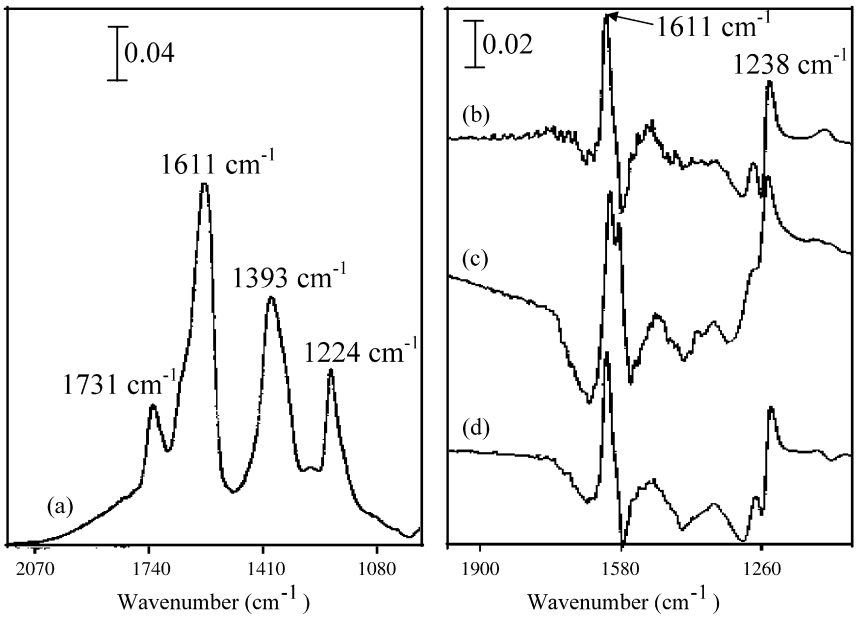

Fig. 9. (left panel) (a) Infrared spectrum of species adsorbed on TiO_2 during photooxidation of TCE at high concentration. (right panel) (b) Infrared spectrum of species adsorbed on TiO_2 by standard phosgene. (c) Species adsorbed during photooxidation of standard adsorbed DCAC at high concentration. (d) Species adsorbed during photooxidation under the conditions shown in the left panel in (a). The oxidation time with UV irradiation for infrared spectra of (c) and (d) was 70 min.

studies are needed to determine the state of chlorine adsorbed on the surface of TiO_2.

3.4. Photocatalytic oxidation of adsorbed DCAC and adsorbed DCAA on TiO_2

As described above, the adsorbed species during photocatalytic oxidation of TCE was newly found to be adsorbed DCAC alone, although the main byproducts were DCAC and phosgene. Fig. 9 shows the infrared spectra of adsorbed phosgene and (a) the species adsorbed on TiO_2 during photooxidation of TCE at high concentration. The infrared bands of standard adsorbed phosgene were observed at 1611 cm^{-1} for the COO asymmetric stretch and at 1238 cm^{-1} for the COO symmetric stretch (as shown in Fig. 9(b)). The species adsorbed during photooxidation of DCAC adsorbed at high concentration, as shown in Fig. 9(c), were also observed at 1611 and 1238 cm^{-1}. The infrared band observed at 1224 cm^{-1} shown in Fig. 9(a) was degraded during photocatalytic oxidation and was newly observed at 1238 cm^{-1}, as shown in Fig. 9(d). The gas-phase [5,31] and adsorbed DCAC both low and high concentrations were converted to gas-phase phosgene during photocatalytic oxidation. Thus, we found that the surface species adsorbed during photooxidation of adsorbed DCAC and during photooxidation of surface species under the conditions shown in Fig. 9(a), was adsorbed phosgene.

On the other hand, DCAA is produced by photocatalytic oxidation of TCE in water [32] and by hydrolysis of DCAC [33].

DCAA also yielded gas-phase phosgene as a byproduct of photocatalytic oxidation observed as infrared bands at 1832 and 1820 cm^{-1}, 1682, 856, and 848 cm^{-1}. In addition, the adsorbed DCAA was also found to be converted to adsorbed phosgene, because infrared bands were observed at 1611 and 1238 cm^{-1} by photocatalytic oxidation on TiO_2.

4. Discussion

4.1. Proposed surface structure of adsorbed DCAC on TiO_2

As it is very difficult to study the adsorbed structure on TiO_2, no complete interpretation has yet been formulated. Several types of adsorbed structure formed on metal compounds have been reported [34–37]. Recently, we proposed the surface structure of adsorbed phosgene [23]. Although Driessen et al. reported the surface structure on TiO_2 during TCE photooxidation [6], their proposal did not sufficiently explain the surface structure. Therefore, we investigated the surface structure of adsorbed DCAC. The split $\Delta\nu = (\nu_{as} - \nu_s)$ parameters indicate stability of COO vibration frequencies. That is, stronger bonds were associated with greater $\Delta\nu$ values [35]. Thus, the infrared bands at 1570 and 1330 cm^{-1} can be attributed to structure mode (I), while those at 1630 and 1220 cm^{-1} can be attributed to structure mode (II) due to the splitting of degenerate vibrations [34].

With photocatalytic oxidation for adsorbed species, we found that adsorbed phosgene was more stable than adsorbed DCAC. Furthermore, the infrared bands of adsorbed phosgene for the COO vibration frequencies were observed at 1611 and 1238 cm^{-1}, while those of adsorbed DCAC were observed at 1611 and 1393 cm^{-1}. Hence, the adsorbed phosgene and adsorbed DCAC were attributed to structure modes (II) and (I), respectively.

In general, the surface species on TiO_2 is usually adsorbed to hydroxyl groups or water by chemical and physical adsorption [38]. Thus, DCAC was adsorbed through reaction with water on the TiO_2 surface (structure III). As peaks for DCAC adsorbed at low concentration were observed at 1611 cm^{-1} for the COO asymmetric stretching vibration, at 1393 cm^{-1} for the COO symmetric stretching vibration, and at 1224 cm^{-1} for the $CHCl_2$ stretching vibration, we propose the adsorbed structure of DCAC on TiO_2 shown in structure (IV) on the basis of structure mode (I).

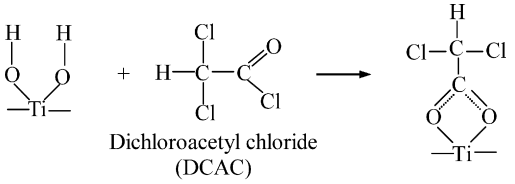

(III) (IV) (5)

In addition, we also investigated the surface structure of DCAC adsorbed on TiO_2 at high concentration, which showed peaks at 1611, 1393 and 1224 cm^{-1}, and also at 1731 cm^{-1} for the C=O stretching vibration. The surface structure of the DCAC adsorbed at high concentration was considered to be formed on DCAC adsorbed at low concentration. Hence, the structure mode (V) shown in reaction (6) was usually adsorbed to hydroxyl groups or water, such as structure (III). Structure mode (V) reacts with gas-phase DCAC, and is subsequently structured to adsorbed DCAC, as shown in structure (VI). The C=O stretching vibration of this structure was observed at the infrared band at 1731 cm^{-1} by FT-IR, and was detected by XPS.

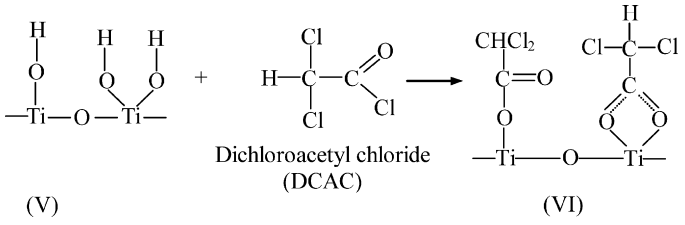

(V) (VI) (6)

This structure, shown as structure (VI), was degraded by photocatalytic oxidation and was subsequently converted to DCAC adsorbed at low concentration as shown in structure (IV). DCAC adsorbed at low concentration was also converted to DCAC adsorbed at high concentration by photooxidation of TCE.

In the case of adsorbed DCAC at high concentration, as there are two types of $CHCl_2$ stretching vibration, as shown in structure (VI), the rate of adsorbed DCAC at high concentration was slower than that at low concentration (Fig. 8). In structures (IV) and (VI), we concluded that the $CHCl_2$ stretching vibration deactivates the photocatalyst.

Furthermore, adsorbed DCAC on TiO_2 was assigned to carboxylate compounds, and adsorbed phosgene was assigned to bidentate carbonate compounds (structure (VII)) accelerating photocatalytic oxidation of TCE in the presence of adsorbed species [23,39]. Eventually, as shown in structures (IV) and (VI), the surface structure of adsorbed DCAC, carboxylate compounds, was converted to that of adsorbed phosgene, bidentate carbonate compounds (structure (VII)), during photocatalytic oxidation under UV irradiation.

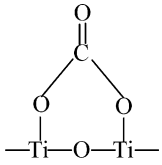

(VII)

On the other hand, the adsorbed DCAA was different from the adsorbed DCAC as follows: (1) DCAA adsorbed on TiO_2, as shown in Fig. 1(d), was degraded more easily than DCAC adsorbed; (2) the band positions of adsorbed DCAA were different from those of DCAC, as shown in Fig. 1; (3) the adsorbed strength of DCAA due to the splitting of degenerate vibrations was weaker than that of DCAC. Therefore, we feel that the surface structure of DCAA was different from that of DCAC. We will investigate the surface structure of DCAA on TiO_2 in the near future.

5. Conclusions

We observed the gas-phase and adsorbed species on TiO_2 during photocatalytic oxidation of TCE. The sole adsorbed species on TiO_2 during TCE photooxidation was adsorbed DCAC. The adsorbed DCAC on TiO_2 was formed to two types of surface structure at low and high concentrations, as shown in structures (IV) and (VI), and was assigned to carboxylate compounds reducing the rate of photocatalytic oxidation of TCE. In structures (IV) and (VI), we considered the $CHCl_2$ stretching vibration to be the inactive species. The adsorbed DCAC at both low and high concentrations was also converted to the adsorbed phosgene by photocatalytic oxidation. Eventually, the surface structure of adsorbed DCAC, carboxylate compounds, was converted to that of adsorbed phosgene, bidentate carbonate compounds (structure (VII)) during photocatalytic oxidation under UV irradiation.

Furthermore, adsorbed DCAA, known to be generated by reaction of water in the presence of DCAC, was also converted to the adsorbed phosgene.

Acknowledgments

The authors would like to thank Prof. Lian-Hua Zhao (Yan Bian University, China) for her insightful comments regarding this study. We are also grateful to Mr. M. Kondo of the Instrumental Analysis Center of Yokohama National University for his skilled assistance with the XPS measurements.

References

[1] J. Kim, K. Itoh, M. Murabayashi, Denki Kagaku 64 (1996) 1200.
[2] K. Hashimoto, T. Watanabe, K. Ishibashi, in: M. Kaneko, I. Okura (Eds.), Photocatalysis: Science and Technology, Kodansha, Tokyo, 2002, pp. 109–121.
[3] L.A. Dibble, G.B. Raupp, Catal. Lett. 4 (1990) 345.

[4] H. Kominami, B. Ohtani, Denki Kagaku 10 (1998) 996.
[5] M.R. Nimlos, W.A. Jacoby, D.M. Blake, T.A. Milne, Environ. Sci. Technol. 27 (1993) 732.
[6] M.D. Driessen, A.L. Goodman, T.M. Miller, G.A. Zaharias, V.H. Grassian, J. Phys. Chem. 102 (1998) 549.
[7] (a) S. Sato, Hyoumen 28 (1990) 427 [In Japanese];
(b) S. Sato, Shokubai 45 (2003) 597 [In Japanese].
[8] S. Yamazaki, T. Tanimura, A. Yoshida, K. Hori, J. Phys. Chem. A 108 (2004) 5183.
[9] P.B. Amama, K. Itoh, M. Murabayashi, J. Mol. Catal. A: Chem. 176 (2001) 165.
[10] M. Murabayashi, Anzen kougaku 40 (2001) 395 [In Japanese].
[11] J. Fan, J.T. Yates Jr., J. Am. Chem. Soc. 118 (1996) 4686.
[12] Y. Luo, D.F. Ollis, J. Catal. 163 (1996) 1.
[13] R. Nakamura, S. Sato, Langmuir 18 (2002) 4433.
[14] K.-H. Wang, J.-M. Jehng, Y.-H. Hsieh, C.-Y. Chang, J. Hazard. Mater. B90 (2002) 63.
[15] M. Schiavello, Heterogeneous Photocatalysis, John Wiley & Sons, Chichester, 1997.
[16] S.-K. Joung, T. Amemiya, M. Murabayashi, K. Itoh, Chem. Eur. J. (2006) in press.
[17] G. Huybrechts, L. Meyers, Trans. Faraday Soc. 62 (1966) 2191.
[18] K. Chhor, J.F. Bocquet, C. Colbeau-Justin, Mater. Chem. Phys. 86 (2004) 123.
[19] K.-H. Wang, H.-H. Tsai, Y.-H. Hsieh, Chemosphere 36 (1998) 2763.
[20] W.A. Jacoby, D.M. Blake, R.D. Noble, C.A. Koval, J. Catal. 157 (1995) 87.
[21] S.-J. Hwang, C. Petucci, C. Raftery, J. Am. Chem. Soc. 119 (1997) 7877.
[22] W. Holden, A. Marcellino, D. Valic, A.C. Weedon, in: D.F. Ollis, H. Al-Ekabi (Eds.), Photocatalytic Purification and Treatment of Water and Air, Elsevier Science Publisher, New York, 1993, pp. 393–404.
[23] S.-K. Joung, T. Amemiya, M. Murabayashi, K. Itoh, Surf. Sci. 598 (2005) 174.
[24] Aldrich Vapor Library of Nicolet 800 FT-IR Spectrometer.
[25] C.R. Bailey, J. Hale, Philos. Mag. 25 (1938) 274.
[26] R.I. Masel, Principles of Adsorption and Reaction on Solid Surfaces, John Wiley & Sons, New York, 1996.
[27] J.S. Brinen, S. Greenhouse, L. Pinatti, Surf. Interf. Anal. 17 (1991) 63.
[28] G. Beamson, D. Briggs, High Resolution XPS of Organic Polymers, John Wiley & Sons, Chichester, 1992.
[29] S.A. Larson, J.L. Falconer, in: D.F. Ollis, H. Al-Ekabi (Eds.), Photocatalytic Purification and Treatment of Water and Air, Elsevier Science Publisher, New York, 1993, pp. 473–479.
[30] A.L. Linsebigler, G. Lu, J.T. Yates Jr., Chem. Rev. 95 (1995) 735.
[31] (a) L.-H. Zhao, S. Ozaki, K. Itoh, M. Murabayashi, Electrochemistry 70 (2002) 8;
(b) L.-H. Zhao, S. Ozaki, K. Itoh, M. Murabayashi, Electrochemistry 70 (2002) 171–173 [In Japanese].
[32] W.H. Glaze, J.F. Kenneke, J.L. Ferry, Environ. Sci. Technol. 27 (1993) 177.
[33] J.-S. Kim, K. Itoh, M. Murabayashi, Chemosphere 36 (1998) 483.
[34] M.L. Hair, Infrared Spectroscopy in Surface Chemistry, Marcel Dekker, New York, 1967.
[35] A.A. Davydov, Infrared Spectroscopy of Adsorbed Species on the Surface of Transition Metal Oxides, John Wiley and Sons, Chichester, 1990.
[36] K. Nakamoto, Infrared Spectra of Inorganic and Coordination Compounds, John Wiley & Sons, New York, 1963.
[37] L.H. Little, Infrared Spectra of Adsorbed Species, Academic Press, London, 1966.
[38] M. Kiyono, Sanka Titan, Gihodo Shuppan, Tokyo, 1991 [In Japanese].
[39] D.V. Kozlov, E.A. Paukshtis, E.N. Savinov, Appl. Catal. B: Environ. 24 (2000) L7–L12.